Prof. Preiswerk. IN.P

To be submitted to
Nuovo Cimento

CERN/TC/PHYSICS 64-30
29.9.1964

THE REACTION $K^+p \rightarrow K^0p\pi^+$ at 3 GeV/c

M. Ferro-Luzzi, R. George, Y. Goldschmidt-Clermont,
V.P. Henri, B. Jongejans, D.W.G. Leith, G.R. Lynch,
F. Muller and J.-M. Perreau,
CERN, Geneva, Switzerland.

CERN LIBRARIES, GENEVA

CM-P00065547

INTRODUCTION

The reaction $K^+p \rightarrow K^0p\pi^+$ has been studied in the 81cm Saclay hydrogen bubble chamber. The separated K^+ beam[1] from the CERN proton synchrotron had a momentum at the centre of the chamber of 2.965 GeV/c (corresponding to a total cm. energy of 2.60 GeV) and a dispersion of 0.015 GeV/c. The pion contamination of the beam was less than 5%.

We find that in this final state the two dominant reactions are

$$K^+p \rightarrow K^{*}p, \quad K^{*} \rightarrow K^0\pi^+ \qquad (1)$$

$$\text{and} \quad K^+p \rightarrow N^{*}K^0, \quad N^{*} \rightarrow p\pi^+ \; . \qquad (2)$$

An analysis of the decay angular distributions of the K^{*} and N^{*} resonances produced in reactions (1) and (2) has been made. In both cases these distributions are consistent with the assumption that the predominant production mechanism is the exchange of a vector meson. A letter containing the main results of this analysis for reaction (1) has already been published[2].

1. EXPERIMENTAL METHOD

Approximately 100,000 bubble chamber photographs, containing $\sim 10^6$ beam tracks, were scanned twice for (among other things) all two-prong V^0 events, i.e. those interactions that had two positive outgoing tracks as well as an associated decay of a neutral particle. A fiducial volume was chosen to eliminate events with large escape corrections and to reduce the number of events with poor resolution. All two-prong V^0 events ($\sim 3{,}000$ events) inside that volume were measured on the CERN IEP measuring projectors. The events were then processed with the CERN computer programs : THRESH (geometry), GRIND (kinematics) and BAKE (calculation of relevant dynamical quantities). All events were then

CERN LIBRARIES, GENEVA

examined to see if the ionization of the tracks was consistent with the kinematic fits and to decide which interpretation to choose in case of ambiguity. Events which failed to pass through THRESH were remeasured; events for which GRIND did not give an answer or for which the wrong interpretation was obtained were processed with MILLSTONE, a program which allows the user to guide GRIND in the performance of the kinematical analysis of individual events.

By means of the above procedure about 99°/o of the true two-prong V^o events were assigned an unambiguous interpretation. The kinematical and dynamical quantities corresponding to the correct interpretations were then selected by the program SLICE and put on a Data Summary Tape, ready to be used by SUMX, a program first developed at Berkeley for the analysis of contents of Data Summary Tapes.

We shall restrict our analysis to the 747 events which fit the reaction $K^+p \rightarrow K^o p\pi^+$. Other types of events fitting $K^oN\pi\pi$ or KKY will be treated in separate papers. By normalizing to the number of τ decays of beam tracks found in the same fiducial volume in which the interactions were analyzed, we find that the cross-section for the reaction $K^+p \rightarrow K^o p\pi^+$ is 2.1 ± 0.3 mb.

2. RESONANCE PRODUCTION

Figure 1 is a Dalitz plot for the $K^o p\pi^+$ events. It can be seen that both the $N^*(1238)$ and the $K^*(890)$ are produced copiously. In order to estimate the relative cross-sections for the K^* and N^* production, we analyzed the Dalitz plot population on the assumption that there are three non-interfering contributions to the $K^o p\pi^+$ final state.

1) $K^+p \rightarrow K^*p$, $K^* \rightarrow K^o\pi^+$, for which the density of events in the Dalitz plot is taken to be[3)]

$$F_{K^*}(M^2_{K\pi};\ M_{K^*},\ \Gamma_{K^*}) = \left[\frac{\Gamma}{\Gamma^2 M^2_{K^*} + (M^2_{K\pi} - M^2_{K^*})^2}\ \frac{M_{K\pi}\ q_p^2}{P_K}\right] \qquad (1)$$

$$\text{with } \Gamma = \frac{P_K^3}{M_{K\pi}}\ \frac{M_{K^*}}{P_o^3}\ \Gamma_{K^*}$$

where M_{K^*} and Γ_{K^*} are the intrinsic mass and width of the K^*, P_K is the momentum of the K^o in the $K\pi$ rest system, P_o is the value of P_K when $M_{K\pi}$ is equal to M_{K^*}, and q_p is the momentum of the proton in the cm. system. This formula is based

on the assumption that the interaction is a quasi two-particle reaction : i.e. that the resonance is produced and decays as a free particle. The formula can be factored into three parts : i) the relativistic Breit-Wigner distribution, $\Gamma / [\Gamma^2 M_{K^*}^2 + (M_{K\pi}^2 - M_{K^*}^2)^2]$, which has only one power of Γ in the numerator because the resonance appears in the final state but not in the initial state of the reaction; ii) the phase space factor $M_{K\pi}/P_K q_p$; iii) the dynamic factor q_p^3, which is appropriate when the resonance is produced via the exchange of a vector meson. The P_K^3 factor in the expression for Γ is a general consequence of a p-wave decay, whereas the $M_{K\pi}$ factor is appropriate for the decay of a vector meson into two pseudo-scalar mesons. The independence of F_{K^*} upon $M_{p\pi}^2$ is a result of a further assumption that the K^* decays isotropically.

2) $K^+ p \rightarrow N^* K^o$, $N^* \rightarrow p\pi^+$, for which the density of events in the Dalitz plot is taken to be[3]

$$F_{N^*}(M_{p\pi}^2;\ M_{N^*},\ \Gamma_{N^*}) = \left[\frac{\Gamma}{\Gamma^2 M_{N^*}^2 + (M_{p\pi}^2 - M_{N^*}^2)^2} \cdot \frac{M_{p\pi}\, q_K^2}{P_p} \right] \qquad (2)$$

$$\text{with} \quad \Gamma = \Gamma_{N^*} \frac{P_p^3}{P_o^3} \left[\frac{(M_{p\pi} + M_p)^2 - M_\pi^2}{M_{p\pi}^2} \cdot \frac{M_{N^*}^2}{(M_{N^*} + M_p)^2 - M_\pi^2} \right]$$

where M_π and M_p are the pion and proton masses and all other quantities are defined analogously to those in the K^* formula. In this case P_o is the value of the proton momentum P_p when $M_{p\pi} = M_{N^*}$.

The factor in brackets in the formula for Γ is the result for N^* decay found from first order perturbation theory.

3) $K^+ p \rightarrow K^o p \pi^+$, for which the events are distributed uniformly in the Dalitz plot. These will be referred to as background events.

The combined Dalitz plot density has the form :

$$L(M_{K\pi}^2,\ M_{p\pi}^2;\ f_{K^*},\ f_{N^*},\ M_{K^*},\ M_{N^*},\ \Gamma_{K^*},\ \Gamma_{N^*})$$

$$= \frac{f_{K^*} F_{K^*}}{A_{K^*}} + \frac{f_{N^*} F_{N^*}}{A_{N^*}} + (1 - f_{K^*} - f_{N^*}) \qquad (3)$$

where f_{K^*} and f_{N^*} are the fractions of events in which K^*'s and N^*'s are produced. The normalization factors are

$$A_{K^*} = \frac{\int F_{K^*} \, dM^2_{K\pi} \, dM^2_{p\pi}}{\int dM^2_{K\pi} \, dM^2_{p\pi}} \quad \text{and} \quad A_{N^*} = \frac{\int F_{N^*} \, dM^2_{K\pi} \, dM^2_{p\pi}}{\int dM^2_{K\pi} \, dM^2_{p\pi}} \; .$$

A likelihood analysis was made on the basis of this distribution to determine the six parameters M_{K^*}, M_{N^*}, Γ_{K^*}, Γ_{N^*}, f_{K^*}, and f_{N^*}. The maximum likelihood solutions for these parameters are presented in Table I. Reactions (1) and (2) are found to proceed with equal rates, each comprising 38 ± 3°/o of the events (corresponding to 0.8 ± 0.1 mb). This leaves 24 ± 3°/o of non-resonant events. Correcting for the K^* decay branching ratio, we find that the cross-section for the reaction $K^+p \rightarrow K^{*+}p$ is about 1.2 mb. The effective mass distributions corresponding to this solution agree fairly well with the data[4], as can be seen in Figures 2 and 3.

This experiment provides an accurate measurement[6] of the mass (891 ± 3 MeV) and width (47 ± 4 MeV) of the K^{*+}. It should be pointed out that the values of M_{N^*}, M_{K^*}, Γ_{N^*} and Γ_{K^*} represent the intrinsic masses and widths of the resonances rather than the experimental positions of the peaks and the experimental widths of the resonances. (These values are also presented in Table I.) Whereas the differences between the intrinsic and the experimental parameters are small for the K^*, the differences are large for the N^*. These shifts are due primarily to the fact that Γ is strongly dependent upon the mass of the resonating system and that Γ appears linearly in the numerator of equations (1) and (2). An additional shift in the same direction is produced by the q^2 factor, but this latter effect is only one MeV in the mass of the N^*. The intrinsic mass (1232 ± 6 MeV) and width (125 ± 30 MeV) of the N^* agree with the values which have been determined from pion-proton scattering data[7]. The position of the peak (1213 ± 4 MeV), as well as the value of the experimental width of the N^*(86 ± 12 MeV) agree well with the values obtained in K^+ experiments at lower energies; for example, at 1.14 GeV/c the values[8] are 1212 ± 8 MeV and 72 ± 13 MeV and at 1.45 GeV/c[9] they are found to be 1214 ± 3 MeV and 100 ± 25 MeV.

In Table II is presented a review of the cross-section measurements that have been made for this reaction at various energies. We note that the cross-section decreases by a factor of five between 2 and 5 GeV/c.

3. ANALYSIS OF THE RESONANCE DECAY DISTRIBUTIONS

For the analysis of the K^* events the 183 events which are in the K^* band (0.86 GeV $< M_{K^0\pi} < 0.94$ GeV) but not in the N^* band (1.15 GeV $< M_{p\pi} < 1.33$ GeV) were chosen. This sample contains $60^0/o$ of the K^* events and has an estimated contamination of 15 background events. For the analysis of the N^*; the 183 events which are in the N^* band (1.16 GeV $< M_{p\pi} < 1.29$ GeV) but not in the K^* band (0.84 GeV $< M_{K\pi} < 0.96$ GeV) were chosen. This sample contains $57^0/o$ of the N^* events and has an estimated contamination of 20 background events. These samples are both designated Sample A. They are illustrated in Figure 4.

It has been demonstrated[10), 11), 2)] that a study of the resonance decay distributions in these reactions can provide some understanding of the production mechanisms involved. It is convenient to analyze these decay distributions in the rest frame of the resonance, choosing the z-axis as the direction of the incident particle (the incident K^+ for the K^* events and the target proton for the N^* events), and the y-axis as the normal to the plane of production. In general, the angular distribution of the K^0 from the decay of the K^* can be expressed in the form[11)]

$$W_{K^*}(\cos\theta, \varphi)\, d\cos\theta\, d\varphi =$$

$$\frac{3}{4\pi}\left[\begin{array}{l}\rho_{0,0}\cos^2\theta + \frac{1}{2}(1-\rho_{0,0})\sin^2\theta \\ -\rho_{1,-1}\sin^2\theta\cos 2\varphi - \sqrt{2}\,\mathrm{Re}\rho_{1,0}\sin 2\theta\cos\varphi\end{array}\right] d\cos\theta\, d\varphi \qquad (4)$$

from which one obtains

$$W_{K^*}(\cos\theta)\, d\cos\theta = \frac{3}{4}\left[(1-\rho_{0,0}) + (3\rho_{0,0}-1)\cos^2\theta\right] d\cos\theta \qquad (4a)$$

$$W_{K^*}(\varphi)\, d\varphi = \frac{1}{2\pi}\left[1 - 2\rho_{1,-1} + 4\rho_{1,-1}\sin^2\varphi\right] d\varphi \qquad (4b)$$

where θ and φ are the polar and azimuthal angles (see Figure 5) and the ρ value are elements in the spin space density matrix of the K^*.

In deriving equation (4) it is assumed that the K^* is a freely decaying particle of spin 1.

Analogously, the angular distribution of the proton from the N^* decay can be expressed in the form[11]

$$W_{N^*}(\cos\theta)\, d\cos\theta\, d\varphi = \frac{3}{4\pi}\left[\rho_{3,3}\sin^2\theta + \left(\frac{1}{2} - \rho_{3,3}\right)\left(\frac{1}{3} + \cos^2\theta\right) - \frac{2}{\sqrt{3}}\mathrm{Re}\rho_{3,1}\sin 2\theta\cos\varphi - \frac{2}{\sqrt{3}}\mathrm{Re}\rho_{3,-1}\sin^2\theta\cos 2\varphi\right] d\cos\theta\, d\varphi \qquad (5)$$

from which one obtains

$$W_{N^*}(\cos\theta)\, d\cos\theta = \frac{3}{4}\left[\frac{1}{3}(1 + 4\rho_{3,3}) + (1 - 4\rho_{3,3})\cos^2\theta\right] d\cos\theta \qquad (5a)$$

$$W_{N^*}(\varphi)\, d\varphi = \frac{1}{2\pi}\left[1 - \frac{4}{3}\mathrm{Re}\rho_{3,-1} + \frac{8}{3}\mathrm{Re}\rho_{3,-1}\sin^2\varphi\right] d\varphi\,. \qquad (5b)$$

In this case the ρ parameters are elements in the spin space density matrix of the N^*, and the N^* is assumed to be a freely decaying particle of spin 3/2.

The parameters $\rho_{0,0}$, $\rho_{1,-1}$, $\rho_{3,3}$, and $\mathrm{Re}\rho_{3,-1}$, were evaluated by a maximum likelihood analysis of the data based on equations (4) and (5). The parameters $\mathrm{Re}\rho_{1,0}$ and $\mathrm{Re}\rho_{3,1}$ were calculated by means of the equations :

$$\mathrm{Re}\rho_{1,0} = -\frac{5}{4\sqrt{2}}\langle\sin 2\theta\cos\varphi\rangle$$

$$\mathrm{Re}\rho_{3,1} = -\frac{5\sqrt{2}}{8}\langle\sin 2\theta\cos\varphi\rangle.$$

The parameters were first calculated using the samples previously described (Samples A). These samples may be biased because in each case some events (about 12 °/o) have been taken away from the sample because they are in the region of the Dalitz plot where the K^* and N^* bands cross. To eliminate this bias we have analyzed the events in the half of the Dalitz plot which does not include this crossing region. Thus (referring to Figure 1), the K^* events are analyzed in the right half, and the N^* events are analyzed in the top half of the plot. More precisely, we have analyzed the events in the region where the cosine of the decay angle[5] of the resonance is negative. These samples are

labelled Sample B. They are illustrated in Figure 4. The events in these samples should also obey equations (4) and (5), when the data are folded in such a way that one plots against $|\cos\theta|$ rather than $\cos\theta$, and against $\varphi \bmod \pi$ rather than φ. In all cases the value obtained for the ρ parameters from this reduced sample are in agreement with the values obtained from the larger sample. In Figures 6 and 7, the θ and φ angular distributions for the K^* and the N^*, respectively, are presented. In each case the data is that of Sample A. As a check, the experimental data for $\cos\theta_{K^*}$ and $\cos\theta_{N^*}$ was also fitted by a polynomial of the form : $y = \sum_{k=0}^{6} a_k \cos^k\theta$, and the χ^2 probabilities compared for different values of $k \leqslant 6$. The best solution was obtained when a polynomial of the form $y = a_0 + a_2 \cos^2\theta$ was used, i.e. additional terms with odd powers of $\cos\theta$ or with $k > 2$ do not improve the χ^2 probability of the fit. This confirms the validity of our a-priori method of analysis.

The parameters obtained from Samples A and B, as well as the final corrected values[12], are shown in Table III.

4. PRODUCTION MECHANISMS

a) Simple one-meson exchange model

We have analyzed the resonance events under the assumption that the production mechanism is one-meson exchange. (Exchange diagrams are illustrated in Figure 8.) This approach is suggested by the fact that for both reactions (1) and (2) the baryon goes strongly backward - relative to the incident K^+ in the centre of mass system, as can be seen in Figures 9 and 10.

In the case of a combination of pseudo-scalar meson and vector meson exchange, the parameter $\rho_{0,0}$ can be given a simple interpretation. Considering first reaction (1), $K^+p \rightarrow K^{*}p$, if there is pion exchange, then, since the particles incident to the K^* vertex are spinless, the orbital angular momentum (ℓ) at this vertex is one, the spin of the K^*. Since the component of the orbital angular momentum in the direction of the incident K^+ (the z-axis) must be zero, the angular momentum of the K^* is described by the spherical harmonic Y_1^0, and the angular distribution of the K^0 relative to the K^+ is proportional to $\cos^2\theta$. If there is vector meson exchange (ρ, ω or φ), conservation of angular momentum and parity again allow only $\ell = 1$. This orbital angular

momentum can couple with the vector meson spin functions S_1^1 and S_{-1}^1, but cannot couple with S_1^o to produce a state of spin one. This gives rise to two terms in the K^* matrix element, one proportional to Y_1^1 and the other proportional to Y_1^{-1}. These terms produce an angular distribution proportional to $\sin^2\theta$. As a result the parameter $\rho_{o,o}$ can be interpreted as the fraction of the events which proceed by way of pion exchange. In the case of pion exchange the distribution in the angle φ is isotropic, whereas it is generally nonisotropic in the case of vector meson exchange. Indeed, φ is exactly the angle used in the well-known Treiman-Yang test[13] for the exchange of a spinless meson. A non-zero value of $\rho_{1,-1}$ places an upper limit upon $\rho_{o,o}$:

$$\rho_{oo} \leqslant 1 - 2 \left|\rho_{1,-1}\right|$$

a relation which can be derived by imposing the condition that the distribution function in equation (4) must not be negative. The quantity $\mathrm{Re}\rho_{1,o}$ is two standard deviations away from zero, large enough to suggest that the one-meson exchange model may not be adequate, but not so large that one is forced to abandon the model.

The striking feature of the K^* data is that the exchange of a single pion does not play a dominant role : within the framework of the simple one-meson exchange model only $7 \pm 6\%$ of the events can be attributed to pion exchange, and the data are consistent with the hypothesis that all of the K^* events proceed via the exchange of a vector meson. It has been pointed out by Gottfried and Jackson[11] that this result does not necessarily indicate that a 1^- meson is exchanged. It only indicates that the parity of the exchanged system is $(-1)^J$, $(J \neq 0)$, where J is the spin of the exchanged system. Assuming the simplest case of a 1^- meson exchange, preliminary results from K^+d and K^-p interactions seem to indicate that the vector meson exchanged in reaction (1) has $T = 0$[14].

The production of the N^* events in reaction (2), $K^+p \rightarrow N^*K^o$, cannot proceed by way of the exchange of a single pion because parity cannot be conserved at a $KK\pi$ vertex. It can proceed via the exchange of a vector meson. In the model of Stodolsky and Sakurai[15], which assumes that the N^* events are dominated by the exchange of a ρ-meson in analogy with the magnetic dipole photoproduction of the N^*, the prediction is that the angular distribution of

the N^{*} decay should be of the form $1 + 3\cos^2\theta'$, where θ' is the angle made by the decay proton with the normal to the production plane. In general, in the system in which the z-axis is the normal of the production plane, the angular distribution, integrated over the azimuthal angle, has the same θ' dependence (in terms of a parameter $\rho'_{3,3}$) as the θ dependence of equation (5a) :

$$W(\cos\theta')\, d\cos\theta' = \frac{3}{4}\left[\frac{1}{3}(1 + 4\rho'_{3,3}) + (1 - 4\rho'_{3,3})\cos^2\theta'\right] d\cos\theta'. \quad (6)$$

Figure 11 is the θ' distribution for the N^{*} events of Sample A. The predictions of the Stodolsky-Sakurai model for the N^{*} decay parameters are listed in Table III.

The angular distributions for the N^{*} events are in satisfactory agreement with the theory of Stodolsky and Sakurai as can be seen in Table III. The θ' distribution is within one standard deviation of the prediction $1 + 3\cos^2\theta'$, and more than three standard deviations from isotropy. The φ distribution is in agreement with the predicted $1 + 2\sin^2\varphi$ distribution and is four standard deviations away from isotropy.

Though we have evidence concerning the determination of the quantum numbers of the exchanged systems, the mass of the exchanged system is not determined. For both K^{*} and N^{*} production the distribution in the momentum transfer is peaked at much smaller values than would be expected from an unmodified one-meson exchange calculation. For the K^{*} production via the exchange of a vector meson, the cross-section is[16]

$$\frac{d\sigma}{d\Omega} = \frac{(\hbar c)^2}{3S}\frac{q'}{q}\left(\frac{f^2}{4\pi}\right)\frac{1}{M_{K^{*}}^2\,(M_V^2 + \Delta^2)^2}\left|F_V(\Delta^2)\right|^2$$

$$\times\left\{\frac{(G_V + G_T)^2}{4\pi}\frac{\Delta^2}{4}\left[(M_K - M_{K^{*}})^2 + \Delta^2\right]\left[(M_K + M_{K^{*}})^2 + \Delta^2\right] + 2S\,q^2 q'^2\sin^2\theta^{*}\left[\frac{G_V^2}{4\pi} + \left(\frac{G_T^2}{4\pi}\right)\frac{\Delta^2}{4M_p^2}\right]\right\} \quad (7)$$

where q and q' are cm. momenta of the incident K^{+} and the outgoing K^{o}, S is the square of the total cm. energy (2.60 GeV), and θ^{*} is the cm. production angle. The parameters G_V and G_T are the vector and tensor coupling constants

for the nucleon vertex, f is the coupling constant for the meson vertex, M_V is the mass of the exchanged vector meson, and F_V is a form factor (assumed arbitrarily, to be the same for vector and tensor coupling). When $F_V = 1$ and M_V equals the ρ mass (.750 GeV), this formula does not agree at all with the data, as can be seen in Figure 9. If the mass of the vector meson is reduced, better agreement with the data can be obtained. But the best fit of this type (corresponding to $M_V = 0.250$ GeV) does not agree very well with the data. Good agreement with the shape of the distribution is obtained by using M_V equal to the ρ mass and using a form factor of the type $F_V(\Delta^2) = e^{-\Delta^2/t^2}$. Corresponding to $G_T = 3.7\ G_V$ (appropriate for ρ exchange), a good fit was obtained to the data for $t = 0.56$ GeV/c. Corresponding to $G_T = 0$ (appropriate for ω exchange) an almost identical solution was obtained for $t = 0.70$ GeV/c. The magnitude of the cross-section was fitted with $\frac{G_V^2 f^2}{(4\pi)^2} = 10$ and 12 for the $G_T = 3.7\ G_V$ and $G_T = 0$ cases, respectively. This latter fit is shown in Figure 9.

For the N^* production the cross-section corresponding to the Stodolsky-Sakurai model is[16]

$$\frac{d\sigma}{d\Omega} = \frac{2(\hbar c)^2}{3S} \frac{q'}{q} \left(\frac{g^2}{4\pi}\right) \left(\frac{G^2}{4\pi}\right) \frac{1}{(M_p + M_{N^*})^2 (M_\rho^2 + \Delta^2)^2} \left| F_V(\Delta^2) \right|^2$$

$$\times \left\{ \frac{\Delta^2}{4} (4M_K^2 + \Delta^2) \left[(M_{N^*} - M_p)^2 + \Delta^2 \right] + \frac{(3M_{N^*}^2 + M_p^2 + \Delta^2)}{M_{N^*}^2} Sq^2 q'^2 \sin^2\theta^* \right\} . \quad (8)$$

Here, q' is the momentum of the N^*, g is the coupling constant at the meson vertex and G is the coupling constant at the baryon vertex. When $F_V = 1$ this formula is also in poor agreement with the data as shown in Figure 10. A good fit is obtained corresponding to $F_V(\Delta^2) = e^{-\Delta^2/(0.72\ \text{GeV/c})^2}$ and $\frac{g^2 G^2}{(4\pi)^2} = 19$.

The quoted values of the squares of the coupling constants have been determined with a precision of about 25°/o from a fit to the shape and to the absolute value of the cross-section.

b) Modified one-meson exchange model

Up to this point the analysis has been made under the assumption that the reactions under consideration are isolated interactions, unaffected by the other K^+p final state channels. A calculation has been made by Gottfried, Jackson

and Svensson[17] that modifies the one-meson exchange model by including absorption effects due to competing processes. These effects are most important for small impact parameters (low partial waves) and produce an appreciable reduction in the production cross-section and a pronounced collimation of the production angular distribution. The K^+p elastic scattering data[18] was used to determine the absorption in the initial state and from it an estimate was made for the absorption in the final states. This modified peripheral model thus attempts to explain, through the absorption, the observed highly peaked production angular distribution without the use of the ad-hoc form factors needed in the simple one-meson exchange model (a)).

In the case of reaction (1), $K^+p \rightarrow K^{*}p$, a fit to the absolute cross-section and its angular dependence was attempted by Gottfried, Jackson and Svensson[17]. For this a mixture of pion exchange and vector-meson exchange was taken. Purely vector-meson exchange gives much too broad a production angular distribution. The pion exchange amplitude is fixed in absolute magnitude by the K^* width and the known πN coupling constant. A solution was obtained by varying the amount of vector-meson (ρ or ω) exchange, the relative sign of the pion and vector exchange amplitudes, and the ratio of tensor to vector couplings in the vector-meson exchange.

The best solution obtained so far by Gottfried, Jackson and Svensson[17] is shown in Figure 9. It predicts a production angular distribution that is much more in agreement with the data than is the prediction given by the simple one-meson exchange model without any additional form factor. The solution also gives the decay correlations and, in particular, predicts the variations of the K^* density matrix elements as a function of the production angle. These variations are represented by the curves on Figure 12a. The density matrix elements reflect the mixture of pion and vector exchange; for example, $\rho_{0,0}$ has a sizeable value at zero angle where pion exchange is most important, and falls towards zero at large angles, as is appropriate for vector exchange.

The experimental density matrix elements show the same trends; this can be seen on Figure 12a, where the events in Sample A have been divided into three momentum transfer intervals with the following limits (in units of $(GeV/c)^2$) :

1) $0.02 < \Delta^2 \leqslant 0.16$
2) $0.16 < \Delta^2 \leqslant 0.36$
3) $0.36 < \Delta^2 \leqslant 0.9$.

Table IV shows the values of the ρ parameters for the events in these three momentum transfer intervals.

The values for $\rho_{o,o}$, $\rho_{1,-1}$, and Re $\rho_{1,o}$, given in Table III, are averages over the production angles. They are in reasonable agreement with the theoretical averages of $\langle\rho_{o,o}\rangle = 0.13$ $\langle\rho_{1,-1}\rangle = 0.31$ and $\langle \mathrm{Re}\rho_{1,o}\rangle = -0.07$.

From the results shown on Figures 9 and 12a we see that for reaction (1), $K^+P \rightarrow K^*p$, the model of Gottfried, Jackson and Svensson[17] can give a reasonable account of the absolute cross-section, the angular distribution of production, and the decay correlations.

For the reaction (2), $K^+p \rightarrow N^*K^o$, a similar calculation was done by the same authors[17], using their modified peripheral model and assuming that the mechanism is the ρ exchange model of Stodolsky and Sakurai[5]. The resultant prediction for the production angular distribution is shown on Figure 10. The experimental values and the theoretical predictions for the parameters $\rho_{3,3}$, $\mathrm{Re}\rho_{3,-1}$ and $\mathrm{Re}\rho_{3,1}$ as a function of production angle are represented on Figure 12b. The predicted average values of $\langle\rho_{3,3}\rangle = 0.27$, $\langle\mathrm{Re}\rho_{3,-1}\rangle = 0.21$ and $\langle\mathrm{Re}\rho_{3,1}\rangle = -0.10$. agree well with the experimental values. However, the agreement on the variation of the ρ parameters with the production angle is only fair.

CONCLUSION

The $K^+p \rightarrow K^o p\pi^+$ events for 3 GeV/c K^+ are composed of $38 \pm 3^o/o$ N^*K^o events and $38 \pm 3^o/o$ K^*p events.

Concerning the production mechanisms of the K^* and N^* we found that :

With-
a)/in the framework of the simple one-meson exchange model, the angular distributions of decay for the K^* events are consistent with the assumption that these events are predominantly produced by the exchange of a vector meson, with only $7 \pm 6^o/o$ of the events being produced by the exchange of a pion. This vector-meson exchange nature has also been observed at lower energies. At 2 GeV/c some vector-meson exchange was noted[19], and for 1.45 GeV/c K^+ it was reported[9] that the ratio of vector to pseudo-scalar-meson exchange is 1.51 ± 0.26. This behaviour of the K^*p events is in sharp contrast with that of the $K^+p \rightarrow K^*N^*$ events, which seem to be dominated by pion exchange[20), 21].

The N^{*} decay angular distributions agree with the predictions of the model of Stodolsky and Sakurai. This was also shown to be the case at lower K^{+} momenta[8), 9)].

For both K^{*} and N^{*} production, using the simple one-meson exchange model, one is unable to fit the very sharply peaked momentum transfer distribution without the use of a form factor of the type $e^{-\Delta^2/t^2}$, with t equal to about 0.6 GeV/c. The need for a form factor to obtain agreement with the data is by no means a peculiarity of these reactions or of vector-meson exchange. For example, such a form factor is also needed in the reaction $K^{+}p \rightarrow K^{*}N^{*}$ [20), 21)].

b) A comparison between theory and experiment for the reactions $K^{+}p \rightarrow K^{*}p$ and $K^{+}p \rightarrow N^{*}K^{o}$ shows that a peripheral model modified to include absorption effects due to competing processes, as done by Gottfried, Jackson and Svensson[17)], can give a reasonable account of the absolute value of the cross-section, the production angular distribution and the decay correlations.

The absorption of low partial waves provide the collimation of the production angular distribution without need of the ad-hoc form factors introduced in the simple one-meson exchange model.

To account for the production of K^{*} in $K^{+}p \rightarrow K^{*}p$, a mixture of pion exchange and vector-meson exchange was used[17)]. The pion exchange is fixed in absolute scale and our results show that a sizeable admixture of vector-meson exchange is needed to fit the observed production distribution.

ACKNOWLEDGMENTS

We have profited from many discussions with Professors J.D. Jackson and K. Gottfried, and Drs. H. Pilkuhn and B. Svensson. Dr. R. Böck has been very helpful in the development of many of the computer programs that we used. Our thanks are due to the crew of the 81cm hydrogen bubble chamber, to the staff of the CERN proton synchrotron and to our scanning staff. We are grateful for the support given to us by Professor Ch. Peyrou.

FIGURE CAPTIONS

Figure 1 A Dalitz plot for the $K^+p \rightarrow K^0p\pi^+$ events.

Figure 2 The projection of the Dalitz plot in Figure 1 onto the $M^2_{p\pi}$ axis. The top curve represents the best fit to the data (corresponding to the parameters given in Table I). The bottom curve is the contribution of the general background. The middle curve represents all events other than the N^* events.

Figure 3 The projection of the Dalitz plot in Figure 1 onto the $M^2_{K\pi}$ axis. The curves are as defined in Figure 2, except that the middle curve excludes the K^* events.

Figure 4 An illustration of the samples used. The A samples include all darkened areas and the B samples are the black areas. The cosine of the decay angle[5] is zero along the curved lines inside the Dalitz plot.

Figure 5 An illustration of the coordinate system in which the angles θ, θ' and φ are defined for the $N^*(K^*)$ events. The symbols p_i and p_f refer to the initial and final state protons. The notation $\vec{P}_{A,B}$ denotes a vector in the direction of the momentum of particle A measured in the B rest frame.

Figure 6 Histograms of the distribution in $\cos\theta$ and φ for the decay of the K^*p events of Sample A. The curves represent the best fit to the data, namely $1 - 0.76\cos^2\theta$ and $1 + 4.3\sin^2\varphi$.

Figure 7 Histograms of the distributions in $\cos\theta$ and in φ for the decay of the N^* in the N^*K^0 events of Sample A. The solid curves represent the best fits to the data, namely $1 - 0.22\cos^2\theta$ and $1 + 1.9\sin^2\varphi$. The dashed curve represents $1 - 0.6\cos^2\theta$, the prediction of the Stodolsky-Sakurai model. For the φ distribution the experimental fit and the predicted curve are almost identical.

Figure 8 Feynman diagrams illustrating the exchange mechanisms which may characterize a) the K^*p events and b) the N^*K^0 events.

Figure 9 A histogram of the cm. angular distribution for the reaction

$$K^+p \rightarrow K^{*}p, \qquad K^{*} \rightarrow K^0\pi^+.$$

Figure 9 (contd.) The curves are according to equation (7). The dashed curve represents no form factor : ($F_V = 1$, $M_V = 750$ MeV, $G_T = 0$); the solid curve represents ($F_V = e^{-\Delta^2/(0.70\ \mathrm{GeV/c})^2}$, $\frac{G_V^2 f^2}{(4\pi)^2} = 12$, $M_V = 750$ MeV, $G_T = 0$). In addition to the statistical errors there is an uncertainty of about 10°/o when the values are interpreted as differential cross-section measurements. The other curve (represented by X's) is a fit according to the model of Gottfried, Jackson and Svensson.

Figure 10 A histogram of the cm. angular distribution for the reaction $K^+p \to N^{*}K^o$, $N^{*} \to p\pi^+$. The curves are according to equation (8). The dashed curve represents no form factor ($F_V = 1$); the solid curve represents ($\frac{g^2G^2}{(4\pi)^2} = 19$, $F_V = e^{-\Delta^2/(0.72\ \mathrm{GeV/c})^2}$). As in Figure 9, there is an estimated systematic error of about 10°/o. The other curve (represented by X's) is a fit according to the model of Gottfried, Jackson and Svensson.

Figure 11 A histogram of the distribution in cos θ' for the decay of the N^{*} in the $N^{*}K^o$ events of Sample A. The solid curve represents the best fit to the data ($1 + 2.4 \cos^2 \theta'$), and the dashed curve represents the prediction of the Stodolsky-Sakurai model ($1 + 3 \cos^2 \theta'$).

Figure 12 A graph of the values of the ρ parameters as a function of production angle obtained from the data in Sample A for (a) the reaction $K^{*}p$, and b) the reaction $N^{*}K^o$. The curves represent the prediction of the model of Gottfried, Jackson and Svensson.

REFERENCES

1) J. Goldberg and J.-M. Perreau, "Un faisceau d'usage général à deux étages de séparation électrostatique au PS" (CERN 63-12, April 9, 1964).

2) G.R. Lynch, M. Ferro-Luzzi, R. George, Y. Goldschmidt-Clermont, V.P. Henri, B. Jongejans, D.W.G. Leith, F. Muller and J.-M. Perreau, Physics Letters, 9, 359 (1964).

3) J.D. Jackson, "Remarks on the Phenomenological Analysis of Resonances", (CERN Preprint TH 416), 1964, to be published in Nuovo Cimento.

4) There is, however, a systematic deviation from this solution. For the projections in both Figure 2 and Figure 3 there are fewer events near the edges than is predicted by the solution. This probably arises principally because the resonances do not decay isotropically as has been assumed. Both have a $\sin^2 \alpha$ component in their decay.

5) The cosine of the decay angle (α) for the K^* and that for the N^* is defined as ($P_{K^o,K^*} \cdot P_{K^*,\,cm}$) and ($P_{p,N^*} \cdot P_{N^*,\,cm}$), where the symbol $P_{A,B}$ denotes a unit vector in the direction of the momentum of particle A measured in the B rest frame, and cm. refers to the overall centre of mass system.

6) As a partial check to determine if there are systematic errors in our mass measurements, we calculated the mass of the K^o, using the unfitted measurements of the decay pions. The resultant value of $M_{K^o} = 498 \pm 2$ MeV indicates that such systematic errors are small.

7) The intrinsic mass (M_{N^*}) of the N^* is defined as the value of the invariant mass of the $\pi^+ p$ system ($M_{\pi p}$) when the phase shift δ_{33} is 90^o. The intrinsic width (Γ_{N^*}) is defined as the value of the width (Γ) when $M_{\pi p} = M_{N^*}$ and Γ is determined from the relation $\cot \delta_{33} = (M^2_{\pi p} - M^2_{N^*})/M_{N^*}\Gamma$. The following table lists some of the values of M_{N^*} and Γ_{N^*} which have been reported from analyses of pion-nucleon scattering data :

Author	M_{N^*} (MeV)	Γ_{N^*} (MeV)
Gell-Mann and Watson (1954) *	1237	116
Anderson (1956) **	1238	123
McKinley (1963) ***	1237 ± 4	112 ± 11
Roper (1964) ****	1234	-

* M. Gell-Mann and K.M. Watson, Annual Review of Nuclear Science (1954), p.219.
** H.L. Anderson, Proceedings of the 6th Annual Rochester Conference on High Energy Physics (1956), Sec. I, p.20.
*** J.M. McKinley, Rev.Mod.Phys. 35, 788 (1963).
**** L. David Roper, Phys.Rev.Letters, 12, 340 (1964).

REFERENCES (contd.)

8) E. Bolt, J. Duboc, N.H. Duong, P. Eberhard, R. George, V.P. Henri, F. Levy, J. Poyen, M. Pripstein, J. Cussard and A. Tran, Phys. Rev. 133B, 220 (1964).

9) G.B. Chadwick, D.J. Crennell, W.T. Davies, M. Derrick, J.N. Mulvey, P.B. Jones, D. Radojicic, C.A. Wilkinson, A. Bettini, M. Cresti, S. Limentani, L. Peruzzo and R. Santangelo, Physics Letters 6, 309 (1963).

10) G.A. Smith, J. Schwartz, D.H. Miller, G.R. Kalbfleisch, R.W. Huff, D.I. Dahl and G. Alexander, Phys. Rev. Letters 10, 138 (1963).

11) K. Gottfried and J.D. Jackson, Physics Letters 8, 144 (1964), and Nuovo Cimento 33, 309 (1964).

12) The principal correction made to the ρ parameters was a correction for background effects. The assumption was made that the non-resonant events are uniformly distributed throughout the Dalitz plot and that the angular distributions of θ and φ for the non-resonant events is also independent of the position in the Dalitz plot. The ρ parameters were calculated for the non-resonant events, treating them as if they were resonant events. These ρ values were then used to correct the ρ values obtained from Sample B. This correction was largest for $\rho_{0,0}$, though even in this case the correction was less than the statistical error. For every parameter the escape correction was very small. In addition, many checks were made to see if there are any biases in the data which might effect the values of the parameters. We find no reason to believe that there are significant biases. In particular, we find that when the K^* peak is divided into a number of mass intervals and the events in each interval are analyzed separately, the data show no mass-dependent effect.

13) S.B. Treiman and C.N. Yang, Phys. Rev. Letters 8, 140 (1962).

14) S. Goldhaber, I. Butterworth, G. Goldhaber, A.A. Hirata, J.A. Kadyk, T.A. O'Halloran, B.C. Shen and G.H. Trilling, "K^+d interactions at 2.3 BeV/c", Paper presented at the 1964 International Conference on High-Energy Physics at Dubna.

R. Barloutand, A. Lévèque, C. Louedec, J. Meyer, P. Schlein, A. Verglas, J. Badier, M. Demoulin, J. Goldberg, B.P. Gregory, P. Krejbich, C. Pelletier, M. Ville, E.S. Gelsema, J. Hoogland, J.C. Kluyver and A.G. Tenner, "$K^- p \rightarrow K^* N$ and $K N^*$ at 3 GeV/c and a comparison between K^+ and K^- reactions" to be published in Physics Letters.

S/4471/mhg

REFERENCES (contd.)

15) L. Stodolsky and J.J. Sakurai, Phys. Rev. Letters 11, 90 (1963).

16) J.D. Jackson and H. Pilkuhn, Nucvo Cimento 33, 906 (1964).

17) K. Gottfried, J.D. Jackson and B. Svensson, "Influence of Absorption due to Competing Processes on Peripheral Reactions", Paper presented at the 1964 International Conference on High-Energy Physics at Dubna and to be published, see also K. Gottfried and J.D. Jackson (CERN Preprint TH 428) to be published in Nuovo Cimento.

18) J. Debaisieux, F. Grard, J. Heughebaert, L. Pape, R. Windmolders, M. Ferro-Luzzi, R. George, Y. Goldschmidt-Clermont, V.P. Henri, B. Jongejans, D.W.G. Leith, G.R. Lynch, S. Muller, J.-M. Perreau, G. Otter and P. Sällström, "K^+p Elastic Scattering at 3.0 and 3.5 GeV/c", Paper presented at the 1964 International Conference on High-Energy Physics at Dubna.

19) S. Goldhaber, Report presented at the Athens Topical Conference on Recently Discovered Particles (1963).

20) M. Ferro-Luzzi, R. George, Y. Goldschmidt-Clermont, V.P. Henri, B. Jongejans, D.W.G. Leith, G.R. Lynch, F. Muller and J.-M. Perreau, Proceedings of the Sienna International Conference on Elementary Particles, Vol. 1, 189 (1963) and to be published.

21) G. Goldhaber, W. Chinowsky, S. Goldhaber, W. Lee and T. O'Halloran, Physics Letters 6, 62 (1963).

TABLE I

Fitted Parameters		Parameters that characterize the experimental distributions	
f_{K^*}	38 ± 3%		
f_{N^*}	38 ± 3%		
M_{N^*}	1232 ± 6 MeV	Peak of N^* mass spectrum	1213 ± 4 MeV
M_{K^*}	891 ± 3 MeV	Peak of K^* mass spectrum	889 ± 3 MeV
Γ_{N^*}	125 ± 30 MeV	Width at half-height of N^* mass spectrum	86 ± 12 MeV
Γ_{K^*}	47 ± 4 MeV	Width at half-height of K^* mass spectrum	46 ± 4 MeV

Maximum likelihood solutions and derived parameters from the analysis of the Dalitz plot population of the $K^o p\pi^+$ events.

TABLE II

p (GeV/c)	E_{cm} (GeV)	$K^o\pi^+p$ (mb)	K^*p, $K^* \rightarrow K^o\pi^+$ (mb)	N^*K^o, $N^* \rightarrow p\pi^+$ (mb)	Ref.
.910	1.745	1.98 ± .2	-	1.9 ± .2	a
1.14	1.849	4.6 ± .3	0.9 ± .3	3.6 ± .5	b
1.45	2.00	4.9 ± .2	2.1 ± .2	2.8 ± .1	c
1.96	2.225	4.6 ± .6	~1.5	~3	d
2.97	2.60	2.1 ± .3	0.8 ± .1	0.8 ± .1	e
3.45	2.78	2.2 ± .3	0.8 ± .1	0.8 ± .1	f
4.97	3.24	1.0 ± .2	0.3 ± .1	0.3 ± .1	f

a) B. Kehoe, Phys.Rev.Letters 11, 93 (1963).

b) E. Boldt, J. Duboc, N.H. Duong, P. Eberhard, R. George, V.P. Henri, F. Levy, J. Poyen, M. Pripstein, J. Crussard and A. Tran, Phys. Rev. 133B, 220 (1964).

c) G.B. Chadwick, D.J. Crennell, W.T. Davies, M. Derrick, J.H. Mulvey, P.B. Jones, D. Radojicic, C.A. Wilkinson, A. Bettini, M. Cresti, S. Limentani, L. Peruzzo and R. Santangelo, Phys. Letters 6, 309 (1963), and private communication from D.H. Locke.

d) S. Goldhaber, Report presented at the Athens Topical Conference on Recently Discovered Resonant Particles (1963).

e) Present paper.

f) Present authors' preliminary results and paper presented at the 1964 International Conference on High-Energy Physics at Dubna.

TABLE III

Parameter	Range	Sample A	Sample B	Corrected value	Stodolsky-Sakurai prediction
$\rho_{0,0}$	0, 1	0.11 ± .05	0.11 ± .06	0.07 ± .06	-
$\rho_{1,1}$	-1/2, 1/2	0.34 ± .04	0.31 ± .06	0.32 ± .06	-
Re ρ_{10}	$-1/2\ \sqrt{2}$, $1/2\ \sqrt{2}$	-0.05 ± .04	-0.09 ± .05	-0.10 ± .05	-
$\rho_{3,3}$	0, 1/2	0.29 ± .05	0.27 ± .06	0.28 ± .06	0.375
Re $\rho_{3,-1}$	$-\sqrt{3/4}, \sqrt{3/4}$	0.21 ± .04	0.21 ± .05	0.21 ± .05	0.216
Re $\rho_{3,1}$	$-\sqrt{3/4}, \sqrt{3/4}$	0.01 ± .04	0.04 ± .05	0.04 ± .05	0
$\rho'_{3,3}$	0, 1/2	0.03 ± .04	0.05 ± .06	0.05 ± .06	0

TABLE IV

Δ^2 intervals $(GeV/c)^2$	$K^+p \rightarrow K^*p$			$K^+p \rightarrow N^*K^0$		
	$\rho_{0,0}$	$\rho_{1,-1}$	$Re\rho_{1,0}$	$\rho_{3,3}$	$Re\rho_{3,-1}$	$Re\rho_{3,1}$
0.02 - 0.16	0.15±0.11	0.23±0.09	-0.06±0.06	0.20±0.08	0.25±0.08	0.12±0.08
0.16 - 0.36	0.14±0.09	0.40±0.07	-0.03±0.06	0.41±0.04	0.12±0.07	-0.02±0.07
0.36 - 0.9	0.00±0.06	0.41±0.07	0.00±0.08	0.22±0.07	0.28±0.07	-0.05±0.07

DIA 20130 FIG 1
PS/4471/mlg

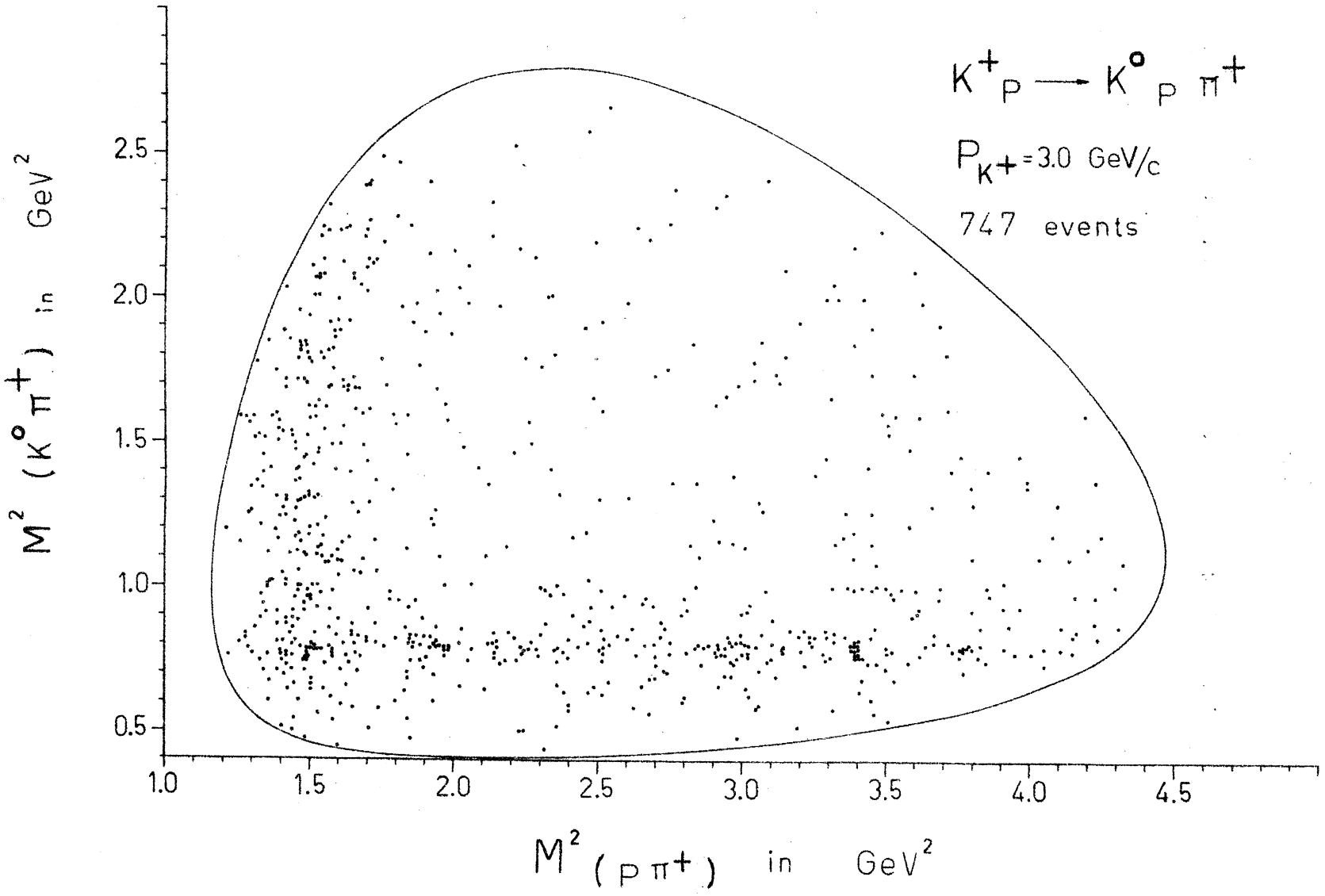

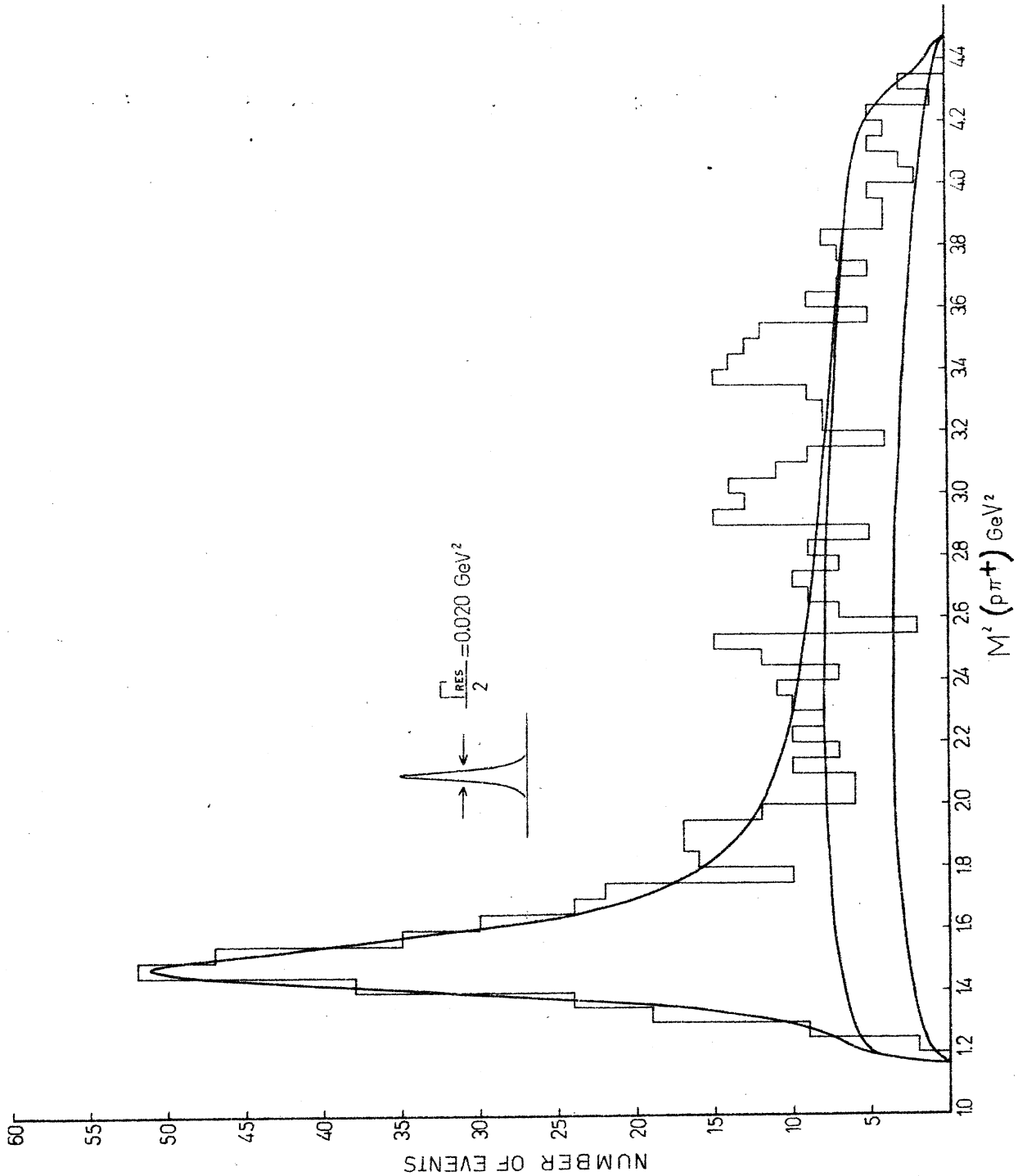

DIA 20147 FIG 2

PS/4471/mlg

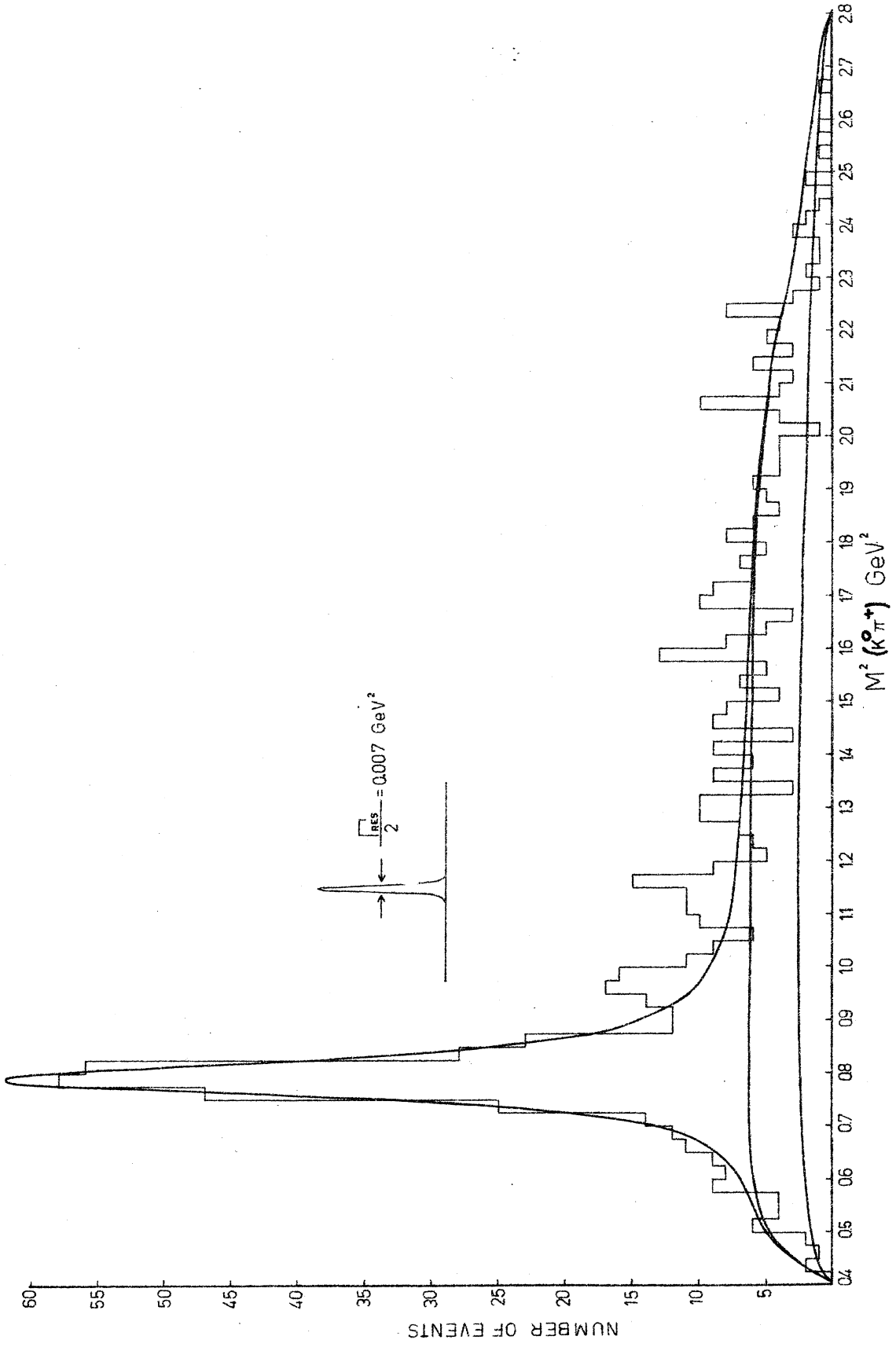

DIA 20148 FIG 3

PS/4477/mlg

DIA 20148 FIG 4
PS/4471/mlg

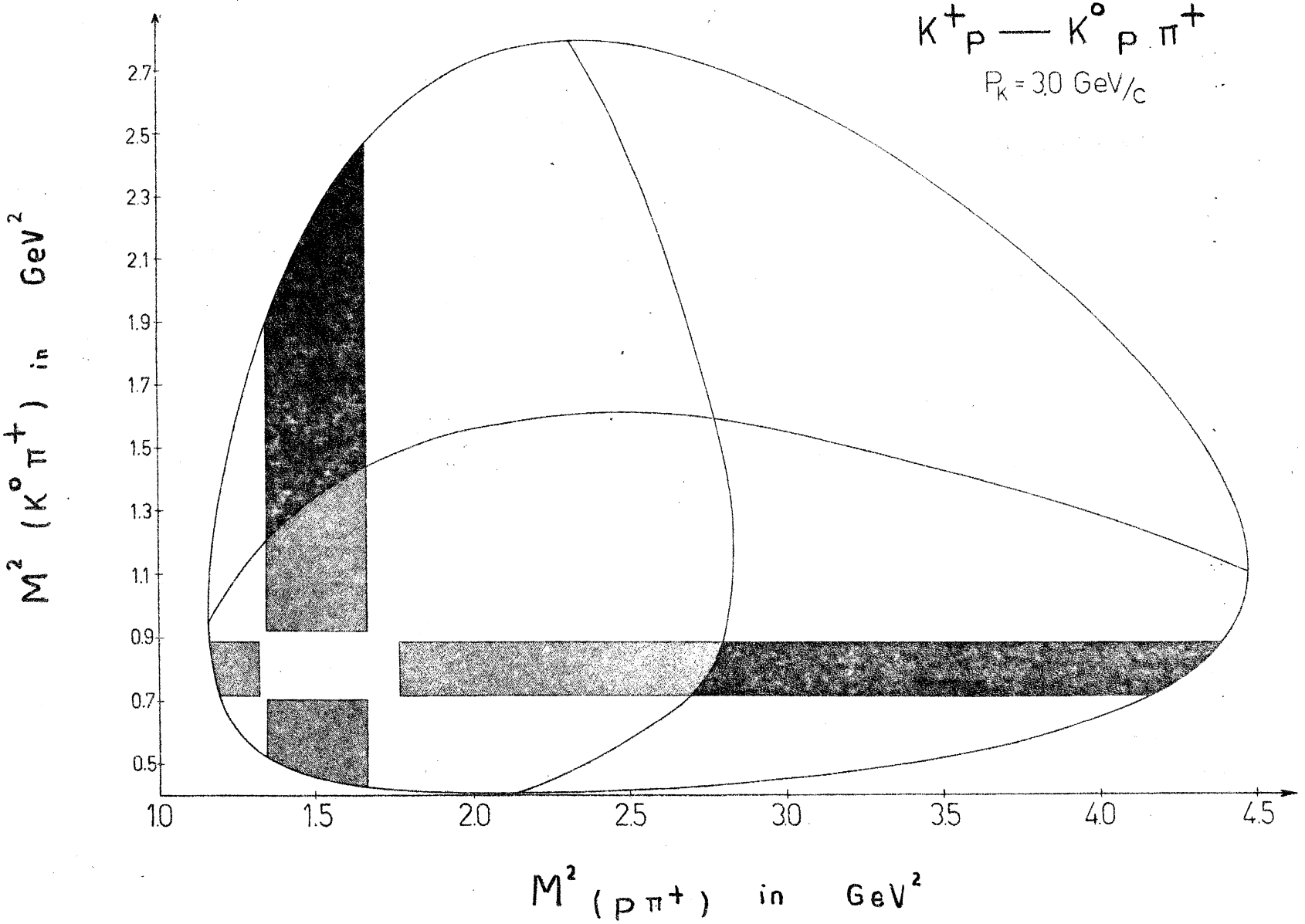

DHA 11825
PS/44471/mlg FIG 5

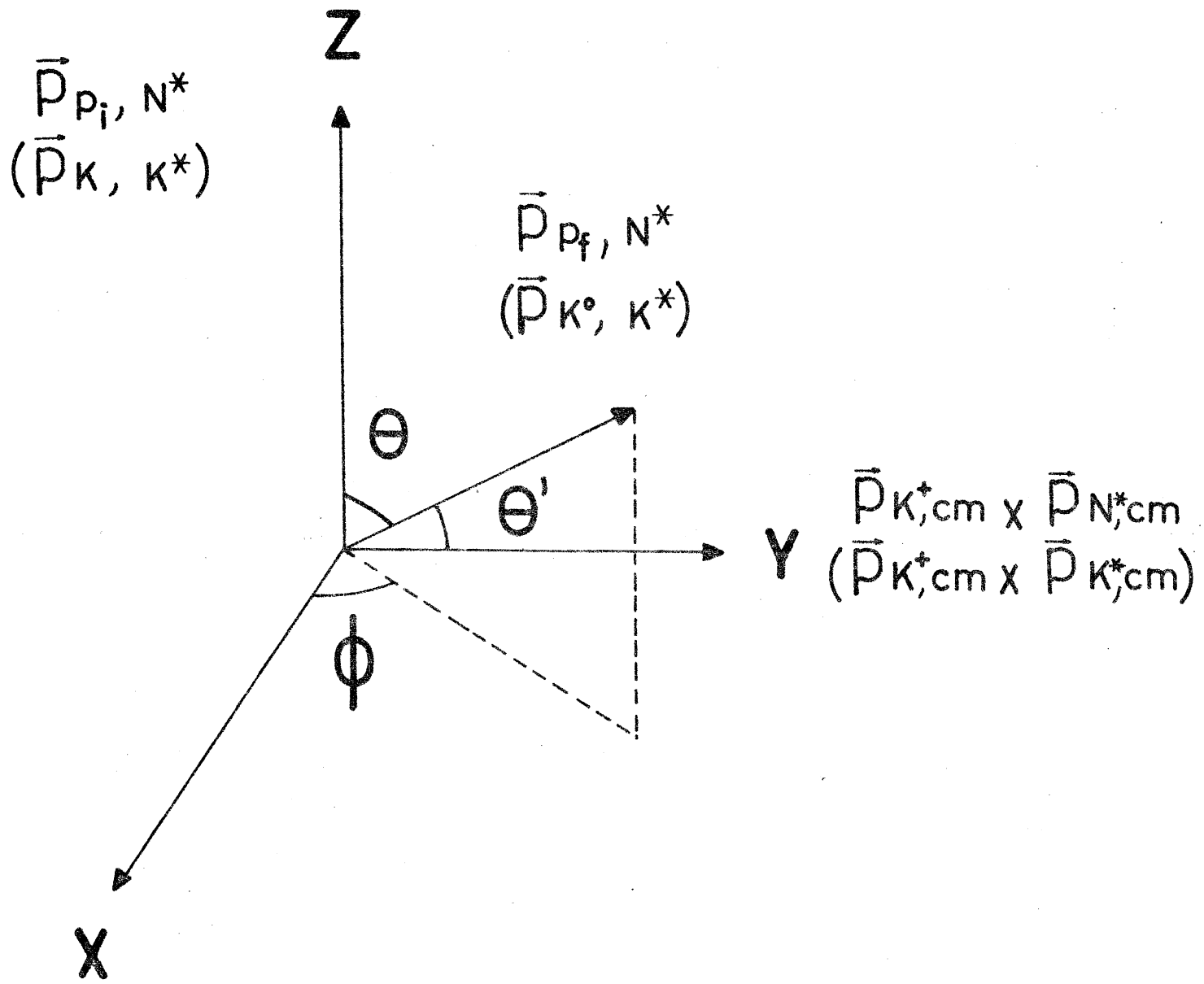

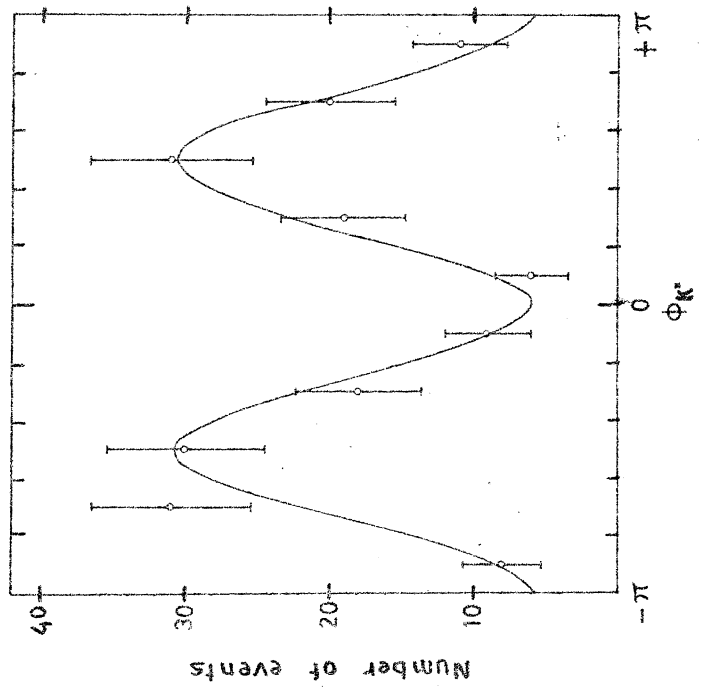

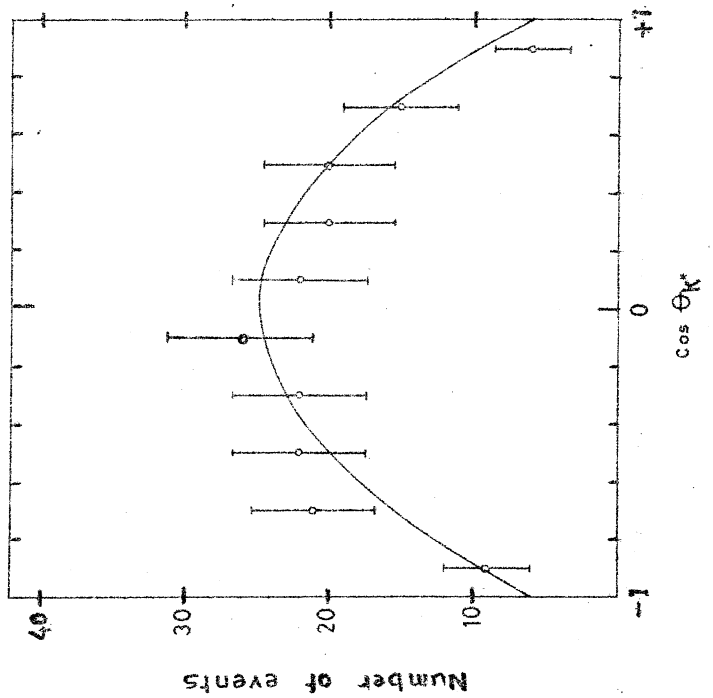

DIA FIG 6

PS/4477/mhg

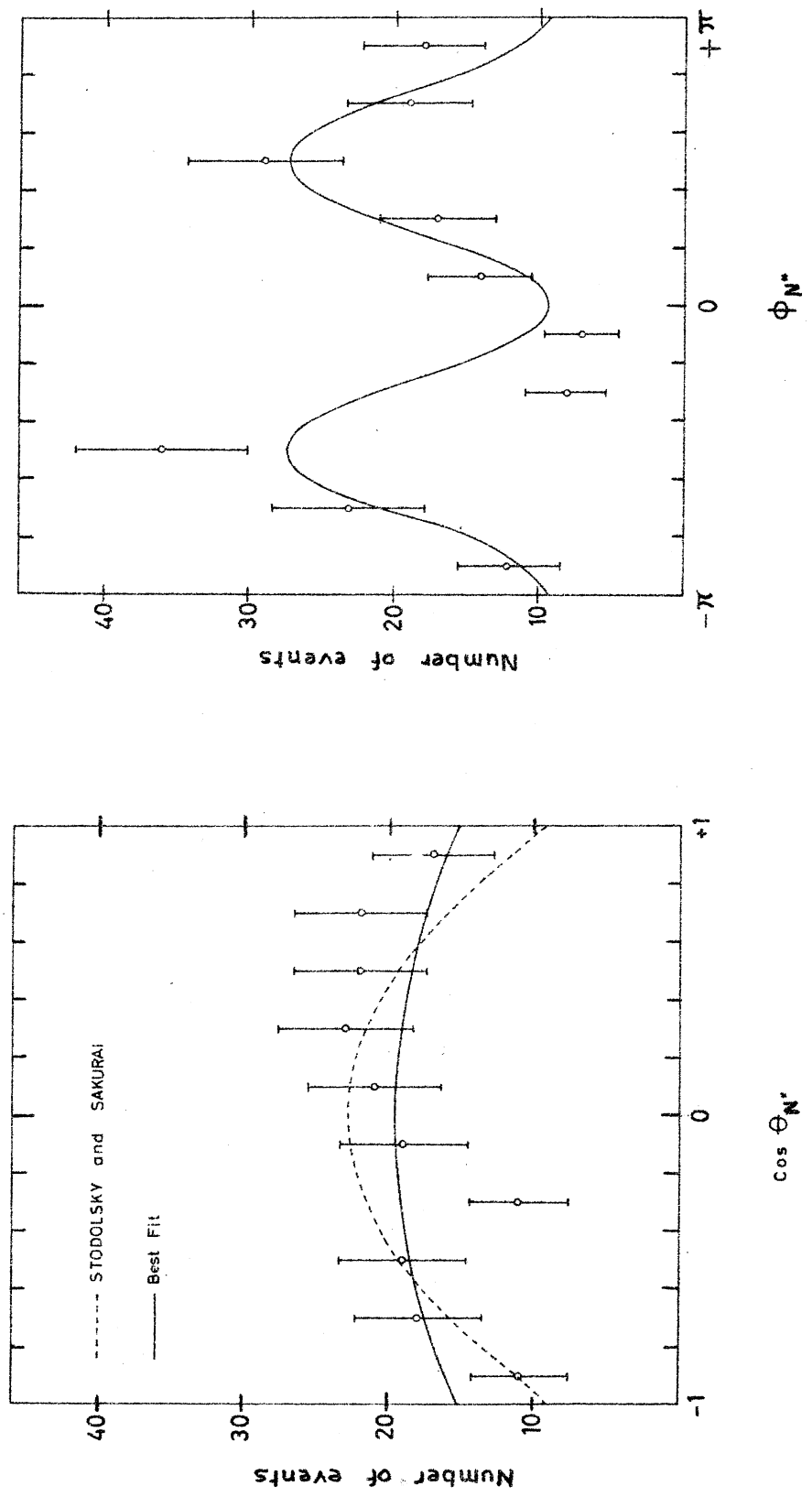

DIA 20150 FIG 7

PS/4477/mlg

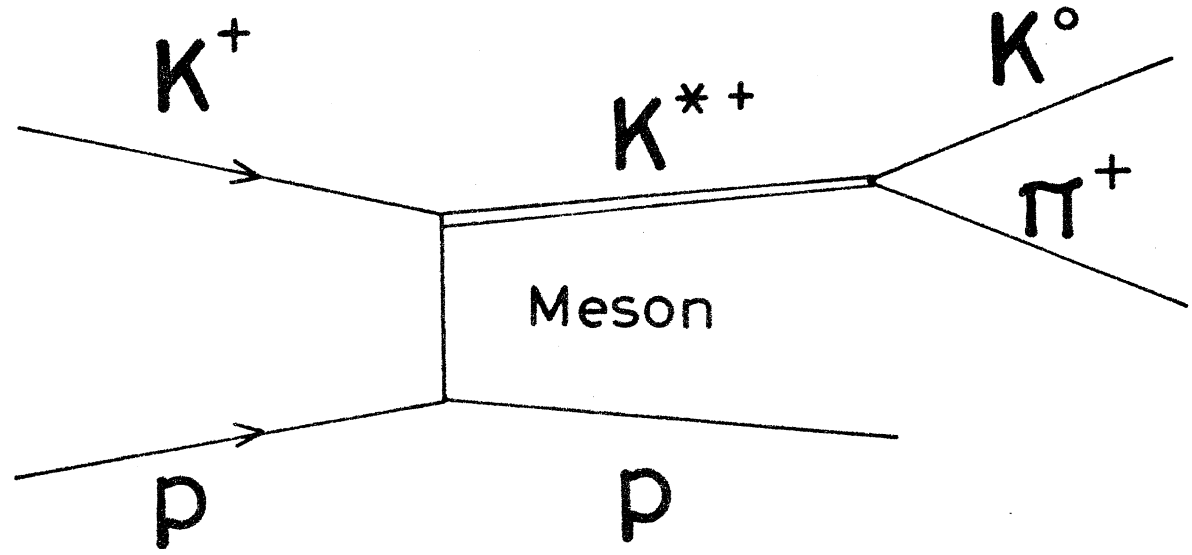

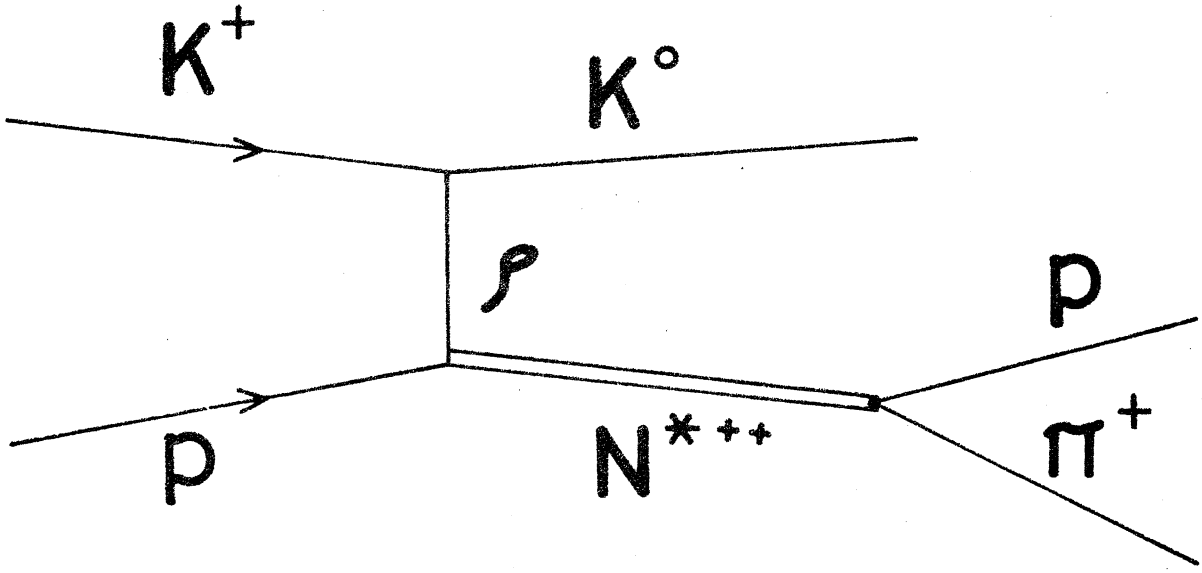

DIA 21326 FIG 8
PS/4477/mdg

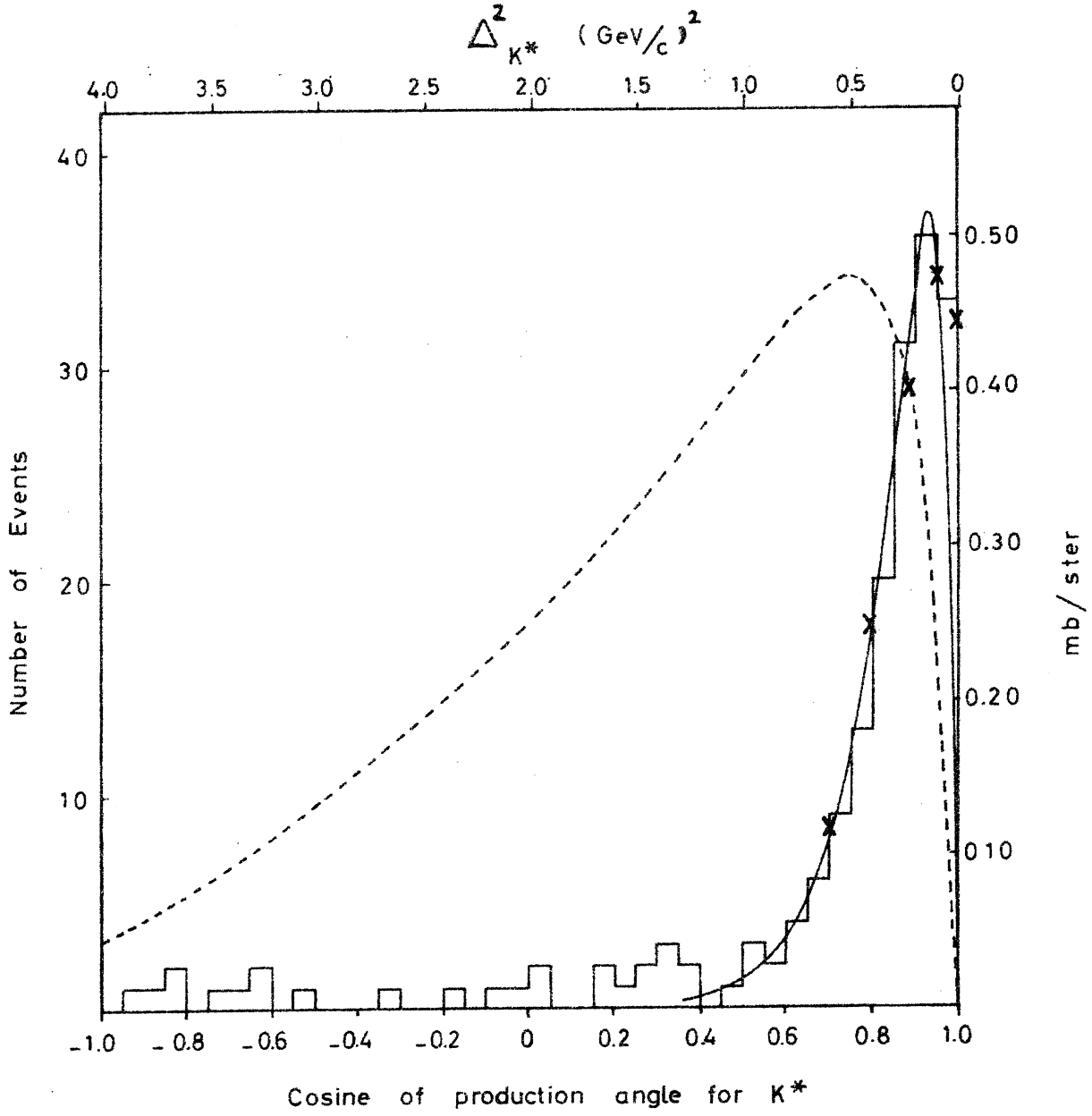

DIA FIG 9

PS/4471/mhg

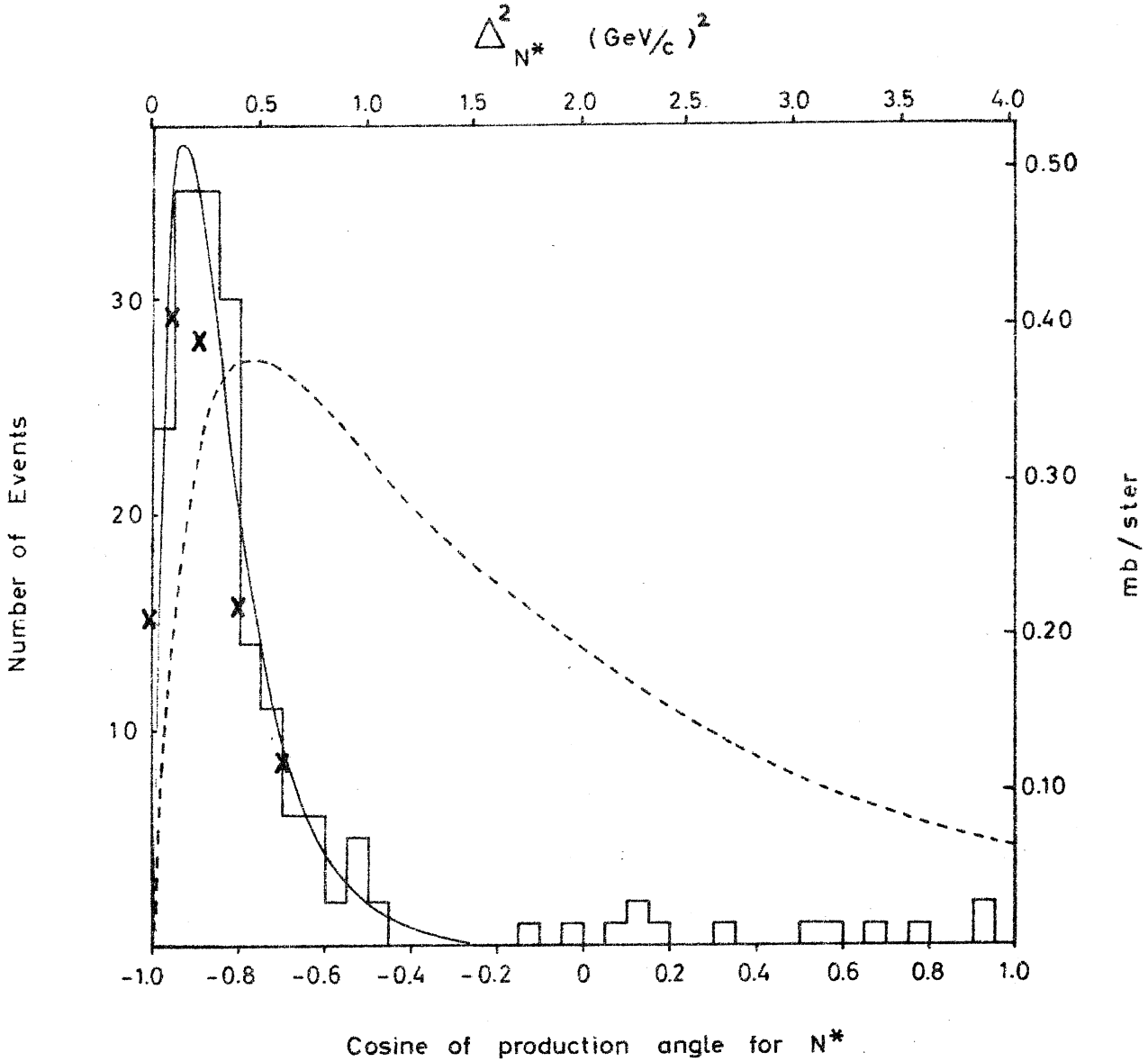

DIA FIG 19

PS/4471/mbg

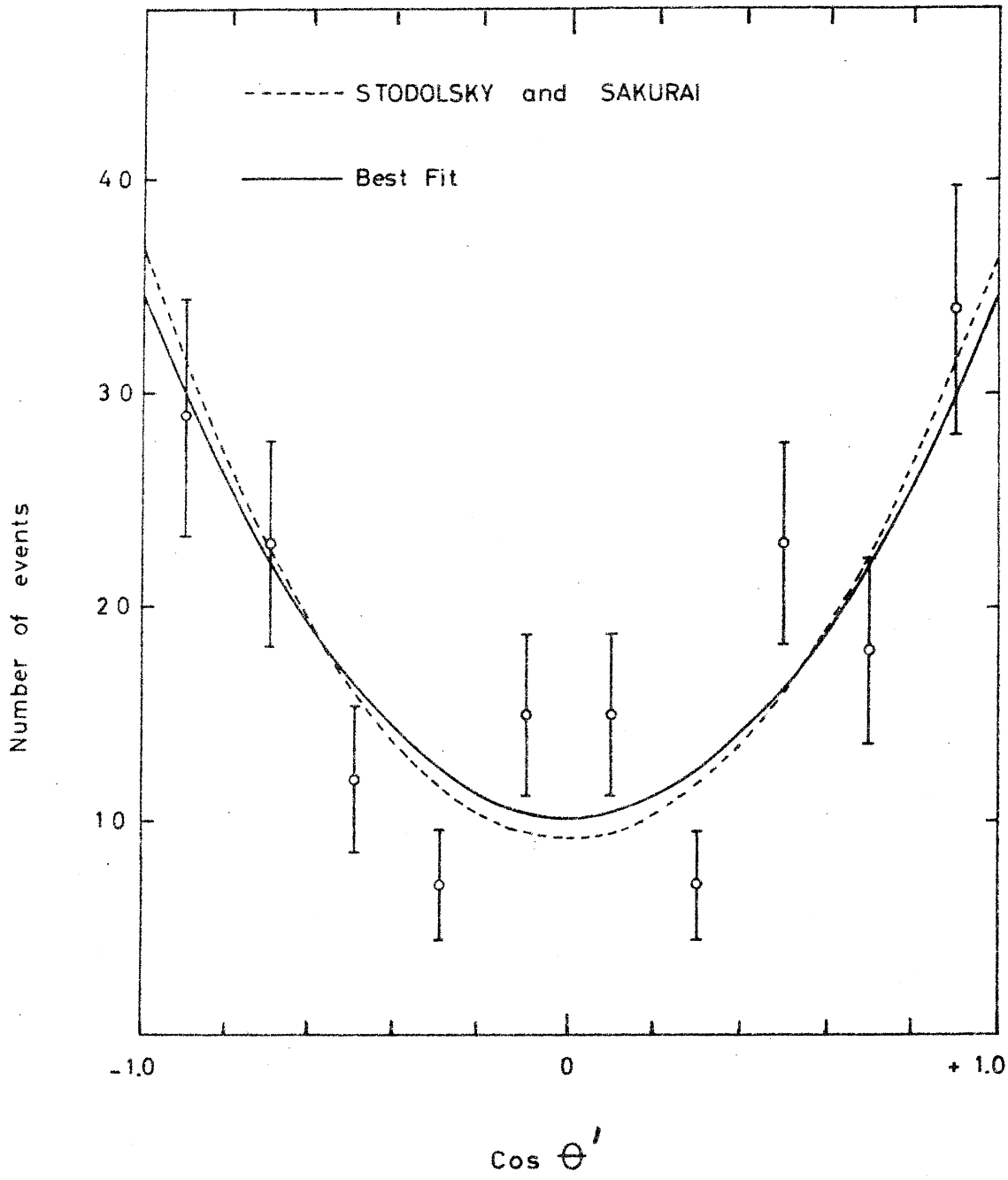

DIA 20145 FIG 11
PS/4471/mhg

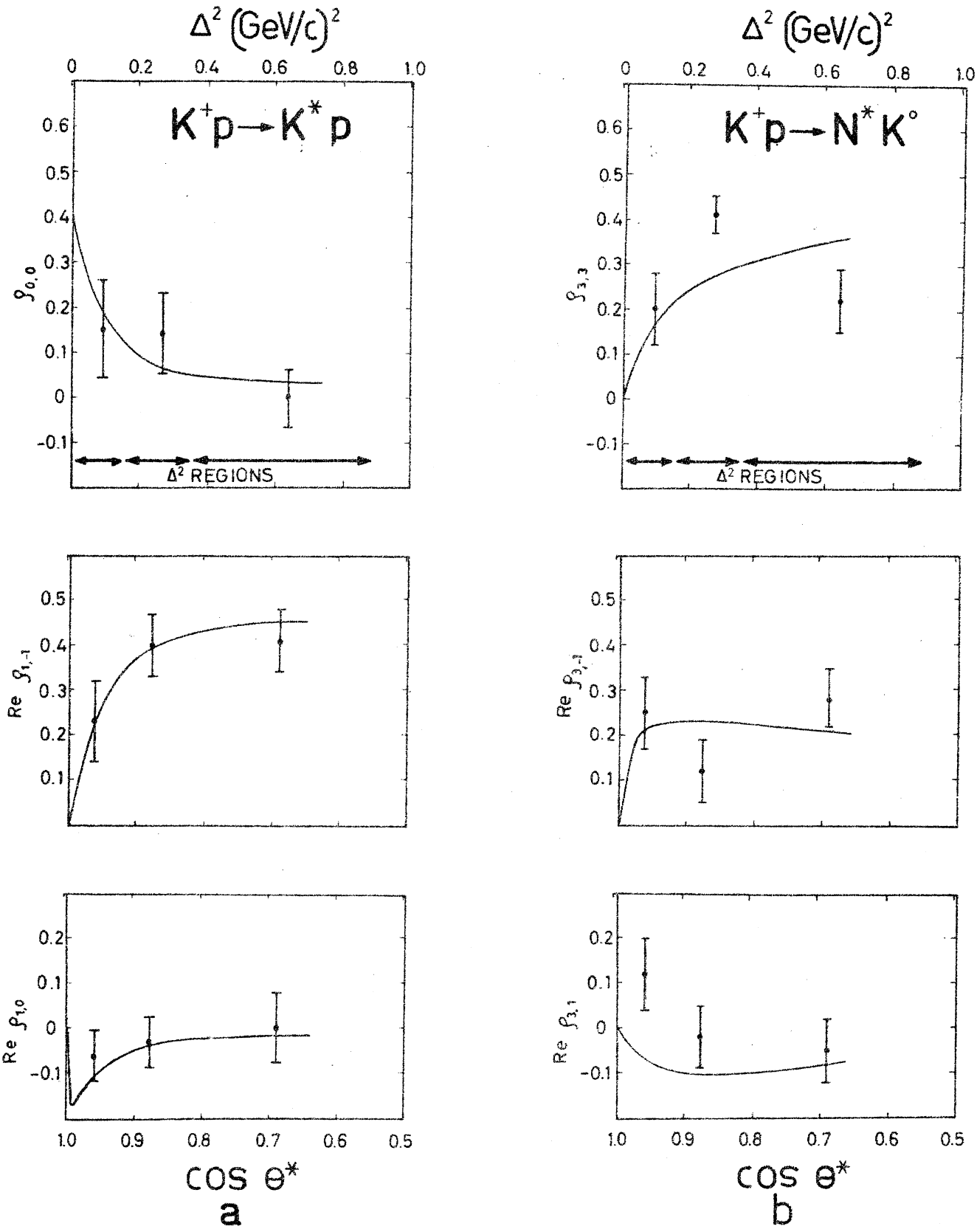

DIA 21618 Fig 12.

PS/4471/mhg